Journal of Advanced Research in Micro and Nano Engineering

Journal homepage:
https://semarakilmu.com.my/journals/index.php/micro_nano_engineering/index
ISSN: 2756-8210

Effect of Filament Pre-Drying on the Microstructure and Porosity of 3D Printed PLA

Rahimah Abdul Hamid[1,*], Siti Hidayah Husni[2], Teruaki Ito[3], Shajahan Maidin[1], Madihah Maharof[4]

[1] Fakulti Teknologi dan Kejuruteraan Industri dan Pembuatan, Universiti Teknikal Malaysia Melaka, 76100 Durian Tunggal, Melaka, Malaysia
[2] Perbadanan Harta Intelek Malaysia, Aras LG, G, 2-5, 11-13 & 15-23, Menara MyIPO, PJ Sentral, Lot 12, Persiaran Barat, Seksyen 52, 46200
[3] Petaling Jaya, Selangor Malaysia
[4] Graduate School of Computer Science & Systems Engineering, Okayama Prefectural University, Soja-shi, Okayama 719-1197, Japan
Department of Mechanical and Production Engineering, Islamic University of Technology Board Bazar, Gazipur-1704, Bangladesh

ARTICLE INFO

Article history:
Received 6 July 2024
Received in revised form 11 August 2024
Accepted 21 September 2024
Available online 31 October 2024

Keywords:
PLA filament; pre-drying; microstructure

ABSTRACT

This paper explored the effect of filament pre-drying before 3D printing. A comparison between the undried and pre-dried 3D printed PLA was evaluated in terms of porosity, microstructure, and polymeric chain bonding. Three conditions were examined: a new PLA as a reference, used PLA filament stored in a vacuumed bag with 50g desiccant, and used PLA exposed to humidity for 48h, 96h, and 150h. The parameter setting for drying and 3D printing was constant for all conditions. As a result, pre-drying the filament resulted in a less porous microstructure, shorter interlayer gap, and better interlayer adhesion. The pre-drying method offers a better microstructure than undried filament. The density of the pre-dried sample was increased as the porosity decreased due to the improvement in the mass flow rate upon the extrusion process. Lastly, the FTIR analysis shows that the pre-dried filament exhibits an O-H molecule free from the O-H region broad peak, which shows no or almost no presence of water (H_2O).

1. Introduction

PLA (Polylactic Acid) is widely used in 3D printing. However, thermoplastic filament like PLA is hygroscopic. Improper storage of the used thermoplastic filaments creates room for moisture absorption, affecting the performance and quality of the printed part. Poor environmental conditions such as humidity may cause warping, poor layer adhesion, and uneven portions [1]. Moisture in the thermoplastic causes the filaments to expand, boil, and break as they are extruded. This may influence surface quality, layer adhesion, and mechanical performance [2,3]. Moisture absorption via the filament increases elongation upon break, lowering elastic modulus and stresses [4]. The absorbed water cluster may lead to the creation of micro cracks, which is thought to be the primary reason for these property decreases.

* *Corresponding author.*
E-mail address: rahimah.hamid@utem.edu.my

https://doi.org/10.37934/armne.24.1.8594

In humid conditions, the strength of the 3D-printed item was decreased due to an aging impact. Absorbing water molecules destroys plastic polymer chains, which produces printing issues [5]. On the other hand, humidity can also influence the mechanical properties of 3D printed parts due to the existence of water by altering the polymer chain's bonding [6]. Drying the filament before printing may be an alternative to eliminate moisture, restore the original performance of the filament, and prevent it from being disposed of as waste, which simultaneously supports sustainability [7,8]. Many researchers were focusing in the optimization of process parameters [9-13], and the exploration in the influence of drying is still limited [14]. Therefore, the present study aims to examine the influence of pre-drying the filament before 3D printing using a dehydrator and the oven on the microstructure of the 3D-printed PLA. The cross-sectional of the PLA specimen was analyzed using SEM.

2. Methodology

2.1 Preparation of the Filament

The materials used in this study were Polylactic Acid (PLA). PLA has a relatively low melting point (150℃-160℃), requiring less printing energy. In this study, different humidified conditions were initially established to expose the filaments to moisture and pre-drying the filament was subsequently performed to observe the drying effect. Three groups were set:

i. New filament as the reference
ii. Used filaments stored in a vacuum bag with 50g desiccant
iii. Used filament stored in an open environment and exposed to a humidifier for 48, 96 and 150 hours

A home humidifier was used for the moisture-exposed condition and a humidity meter was used to measure the humidity level during the exposure.

2.2 Pre-Drying Process

The drying process must be done below the filament's melting point to restore its mechanical properties. Therefore, the drying temperature is a critical factor to consider. High drying temperatures can lead to crystallization and hardening, which may reduce the material's flexibility during 3D printing. In this study, a dehydrator, and an oven, as shown in Figure 1, were used for the drying technique. The temperature was set to 50℃, and the duration was 6 hours, respectively.

(a) (b)

Fig. 1. Two different methods used for the filament pre-drying; (a) Oven, (b) Dehydrator: SUNLU FilaDryer S1

2.3 3D Printing

A few setting parameters were set to follow during the printing process, and the process parameters remained the same for all three conditions of the filaments used. For printing temperature, the optimum setting depends on the filament material used. An incomplete crystalized process causes the printed sample to have a low cooling rate. It affects the samples' strength because the material requires efficient time to ensure it is wholly crystallized [15]. Hsueh *et al.,* [16] suggested that the recommended printing temperature range for PLA filaments is 190℃ to 220℃. As for the printer speed, a lower printer speed was more efficient in providing better-finished output and better-quality results. PLA printing was typically fine at any speed from 40mm/s to 70mm/s. Bed temperature significantly allows materials to cool slower when extruded to prevent warping. It also gives added adhesion, meaning that the first layer holds well during printing, and the component was not released from the bed. For this study, the bed temperature was adjusted at 60°C according to the Ultimaker Cura software. Besides, the effect of layer thicknesses is more readily visible when viewing print time and surface finish. The recommended layer thickness recommended by Ultimaker Cura software is 0.1 mm. Besides, most researchers use 0.1 mm as their layer thickness to get a better-quality part. Other than that, a 100% filling percentage was adapted for a great result of mechanical resistance and quick printing [17]. The process parameters for printing the PLA specimens were set according to Table 1.

Table 1
Process parameters for 3D printing

Parameter	Target value
Nozzle temperature	220℃
Bed temperature	60℃
Speed	60mm/s
Infill density	100%
Layer height	0.1 mm

2.4 Scanning Electron Microscope (SEM)

The microstructure of any material has a significant impact on the material's strength. The microstructural analysis is critical to determining how and why a fractured surface degrades. This work examines the fracture cross-sectional surface of the specimen. A Carl Zeiss Evo 50 scanning electron microscope (SEM) with an acceleration of 15 kV was utilized at 50-time and 100-time magnification power.

2.5 Fourier Transform Infrared (FTIR)

FTIR spectroscopy was performed on all samples. Several samples were tested. Isopropanol was used to clean the equipment thoroughly. Therefore, background data was gathered before collecting sample spectra since the findings might be impacted by human breath and air. Printed samples with the dimension of 10mm x 10mm were used for FTIR testing. Figure 2 shows the FTIR machine used in this study.

Fig. 2. Jasco FT/IR-6100 machine

2.6 Porosity Test

The Archimedes principle was used to determine the filament's porosity. A densimeter was used for the measurement. Each sample was tested three times in both air and water. Measurements were taken once the scale had been re-calibrated. After the scale reached equilibrium, each measurement result was recorded. A density formula in Eq. (1), referred to Ning *et al.,* [18] is used for the calculation.

$$\rho = \left(\frac{M_a}{M_a - M_w}\right)\rho_W \quad (1)$$

where M_a is mass of the sample measured in air, M_w is the mass of the sample measured in water and the density of water, ρ_w is 0.1g/cm^3.

3. Results

3.1 SEM Analysis

Examining the SEM images of the surface of the PLA fracture reveals the humidity effect of the specimen with different humidity exposure. Scanning electron microscopy was used to characterize the morphological characteristics of the blend, and poor adhesion was observed at the interface between blend components. Figure 3-5 shows SEM images of the groups. The cross-sectional tensile fractured surface of the reference offers fewer voids, a smooth surface, good interlayer adhesion, and shorter interlayer gaps compared to the longer humidified filaments (150 hours) for both undried and pre-dried samples. Based on these images, the pre-dried samples exhibit a smooth surface and fewer voids than the undried samples, and the reference group portrays better layer adhesion than the other groups.

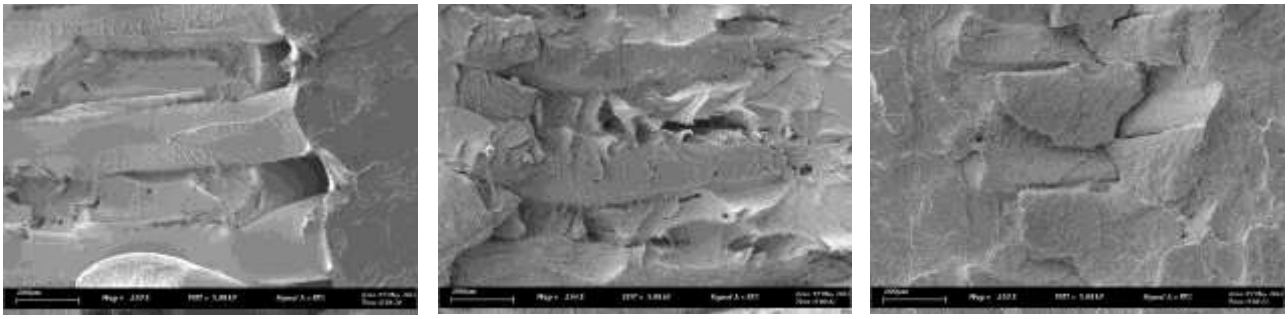

(a) (b) (c)

Fig. 3. SEM images of the reference group; (a) Undried, (b) Dehydrator, (c) Oven

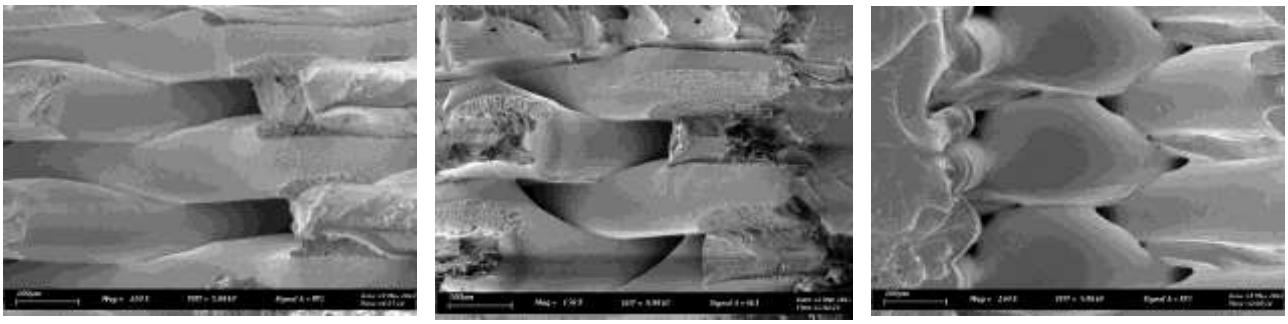

(a) (b) (c)

Fig. 4. SEM images of the used filament stored in vacuum bag with 50g silica gel; (a) Undried, (b) Dehydrator, (c) Oven

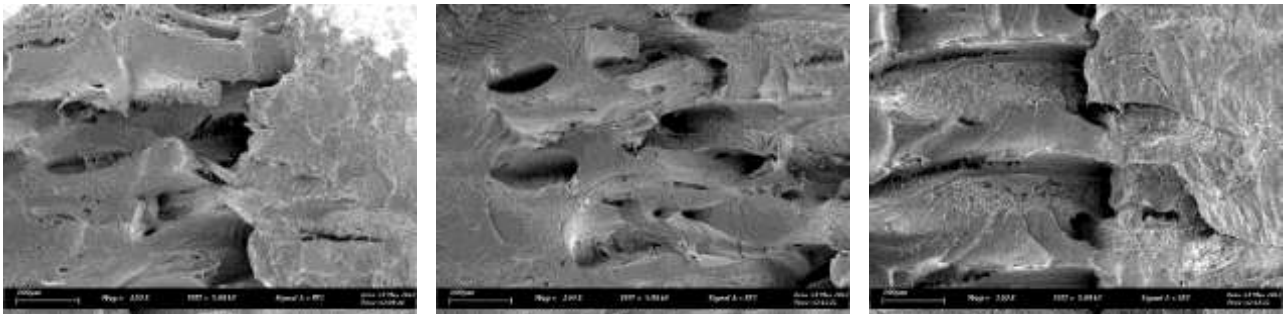

(a) (b) (c)

Fig. 5. SEM images of the 150 hours humidified filament;(a) Undried, (b) Dehydrator, (c) Oven

In addition, the SEM images were subsequently measured using J-image software. Table 2 exhibits the result. The interlayer layer gap for specimens exposed to moisture for 150 hours has the most extended length of a gap for both undried and pre-dried samples. The interlayer gap for the undried specimens is greater than that for the pre-dried specimens utilizing the dehydrator and oven. The reference group had the smallest interlayer gap, and the undried specimens showed more interlayer gaps. On the other hand, the filament used in a vacuum bag with 50g desiccant also exhibits larger interlayer gaps than the samples that have been pre-dried for both methods. This demonstrates that the interlayer gap is optimized when the filament is pre-dried using a dehydrator or oven.

Table 2
Interlayer gap length of the specimens

Specimens	The average length of interlayer gap (μm)		
	Undried	Dehydrator	Oven
New filament (reference)	60.67	26.42	52.17
Used filament stored in the vacuum bag with 50g desiccant	67.42	64.73	44.53
Humidified for 150 hours	99.21	78.28	88.59

3.2 FTIR Analysis

There will be a focus on the hydroxyl absorb area (3650-3200 cm-1), the carbonyl absorbs region (1850-1650 cm-1), and the spectra modified in these three regions because of thermoplastic filaments' effect on the drying process structure alteration. The different absorbance of the peak represents the water absorbance in the filament. The humidity and absorbance in hydroxyl and carbonyl were directly proportional; when the filament humidity increased, the absorbance of the specimen increased as well. A carbonyl stretching vibration is indicated by absorption spectra in the

1850 – 1650 cm-1 (Figure 6). The drying process increases absorption near this position, attributed to the aliphatic carbonyl species from aliphatic carboxyl acids, ketones, or aldehydes for undried specimens. After drying, the absorbance at 1650 and 3350 cm-1 is steady. For example, drying has increased absorption at 1650 cm-1 while decreasing specimens' humidity (dehydrator) and (oven). After drying for six hours on the dehydrator, the absorption at 1723 cm-1 is assigned to the stretching vibration of carbonyl in the ester group of PLA, indicating that no carbonyl group forms in PLA molecules during the drying process.

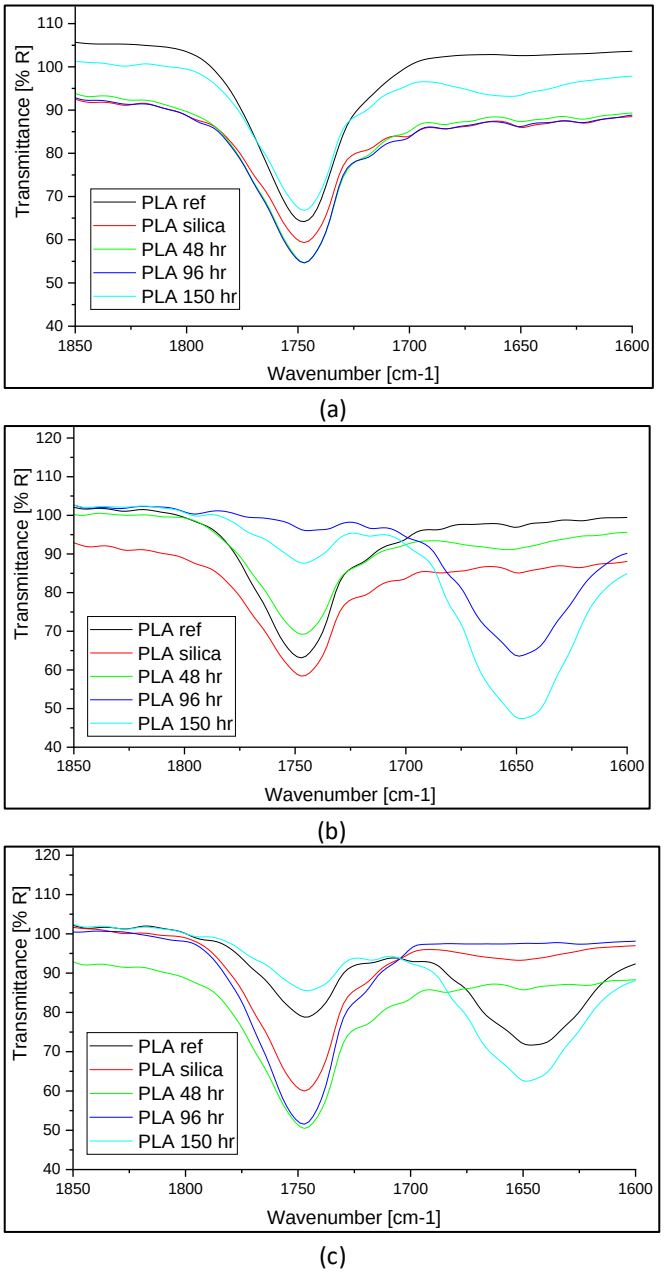

Fig. 6. Carbonyl (CO) absorb region; (a) undried, (b) pre-dried (dehydrator), (c) pre-dried (oven)

The undried specimens show almost no absorption near 3350 cm-1. In contrast, the drying specimens show absorption at this position. With the drying process, the absorption intensity increases, as if the absorb peaks at 3350 cm-1 gradually form, which is assigned to the multiple contributions from the alcohol and acid groups. Furthermore, the peaks at 3350 cm-1 grow

progressively as the humidity of the specimen decreases, showing that no hydroxyl groups are generated during the drying process and that the H_2O is reduced during drying (Figure 7). Still, absorption at 1750 cm-1 in PLA specimens is due to carbonyl stretching vibrations in ester groups.

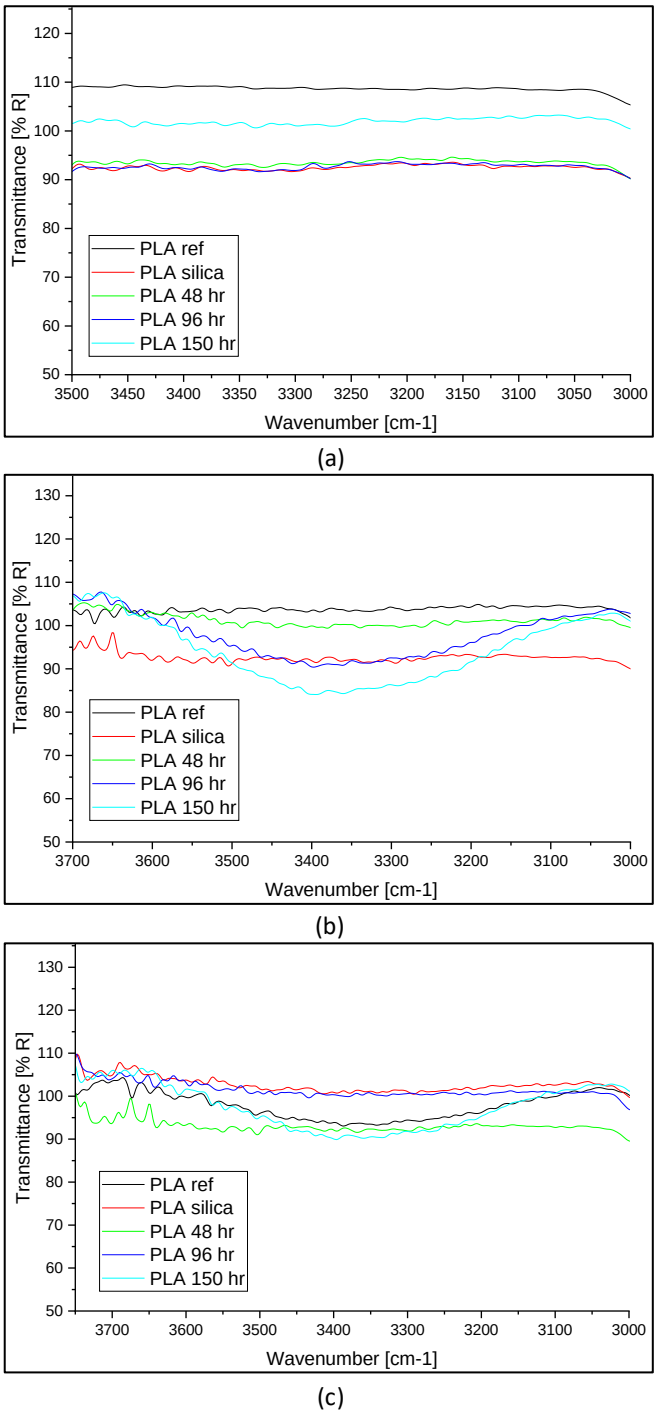

Fig. 7. Hydroxyl (OH) absorb region; (a) undried, (b) pre-dried (dehydrator), (c) pre-dried (oven)

3.3 Porosity Analysis

Based on the density test result in Table 3, the density decreases when the filament is exposed to the humidifier, indicating that when the humidity of the filament increases, the thickness of the

specimen decreases, and the pores or voids in the specimens are higher. Ayrilmis *et al.,* [19] also suggested that the specimen's density decreased, and the porosity in the specimens increased. The density of the PLA filament for undried specimens is lower than for the dehydrator and oven-dried specimens. This indicates that the drying process has reduced the filament's water absorption. This can be explained by the fact that the specimen's porosity increases with water absorption. The filament appears to have a void. It should be noted that closed pore development at moisture content could result in density deviation. However, the difference between measuring particle density and model prediction could be used to quantify the contribution of closed pored to bulk density [20,21].

Interbead pores or interlayer gaps are the most significant flaw in FDM material and the primary source of its mechanical property variability [22]. It may be seen on the fractured surface. Low-strength specimens clearly show the deposited interlayer gap, indicating that the layer was not in contact. The heated bed, which improves bead fusing, is likely responsible for the early layers' low inter-bead porosity. Dimensional variations in the inter-bead voids or pores led to changes in mechanical characteristics. The specimen's interlayer gap length is the subject of this study. A greater interlayer gap indicates that the specimen has high porosity. According to Fang *et al.,* [1], the volume of the biggest pores increases as water content increases, consistent with the findings. As predicted by the fracture process, this experiment demonstrated that specimens with high porosity and low density will have reduced mechanical strength due to the pores' ability to aid crack propagation. Based on the density result, the porosity was calculated, and it was found that the porosity percentage of the specimen was inversely proportional to the density.

Table 3
Interlayer gap length of the specimens

Specimens	Average density (g/cm^3)			Average porosity (%)		
Humidity condition	Undried	Dehydrator	Oven	Undried	Dehydrator	Oven
New PLA filament	1.035	1.042	1.054	16.53	15.97	15.00
Used filament stored in the vacuum bag with 50g desiccant	1.0333	1.038	1.034	16.67	16.29	16.61
Humidified for 48 hours	1.0265	1.029	1.031	17.22	17.02	16.85
Humidified for 96 hours	1.008	1.015	1.025	18.71	18.15	17.34
Humidified for 150 hours	1.0013	1.005	1.005	19.25	18.95	18.95

Figure 8 shows the summarized average density result obtained after the density test to determine each specimen’s average porosity condition. The specimen’s highest average density is obtained in a reference specimen. The specimens with conditions used filament humidified for 150 hours show the lowest strength. Pre-dried specimens have consistently had the highest average density compared to undried specimens. For PLA, pre-dried using a dehydrator shows higher tensile strength than pre-dried using an oven. The new filament specimens have the highest average density, and the specimens with the condition of a humidified filament for 150 hours have the lowest density.

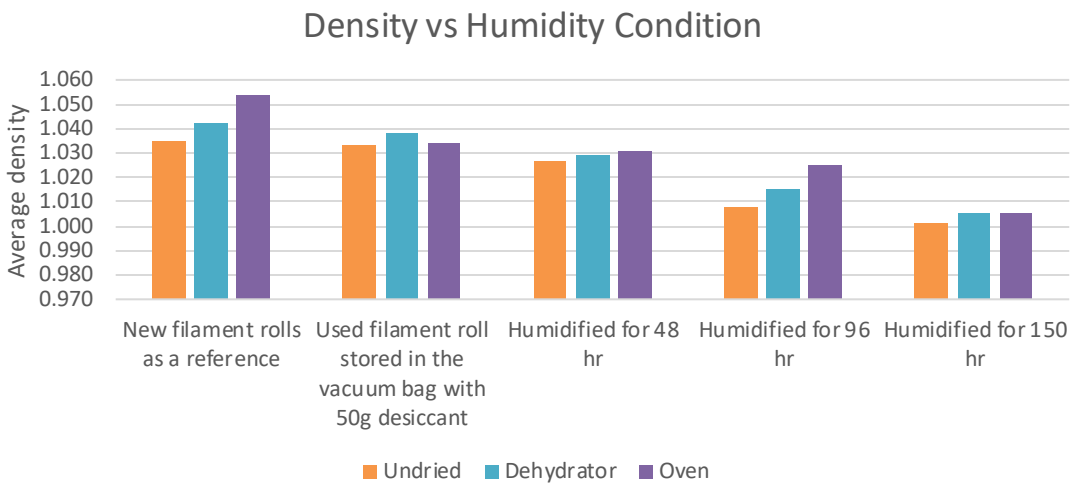

Fig. 8. Average density

4. Conclusions

To conclude, the density of the pre-dried sample was increased as the porosity decreased due to the improvement in the mass flow rate upon the extrusion process. The undried sample exhibits more void and incomplete diffusion in the SEM images, and the interlayer gap expanded due to the moisture. As for the pre-dried sample, the sample had fewer voids and incomplete diffusion, and the layer formation of the dried sample was better than the undried sample. The FTIR analysis of the pre-dried filament shows O-H molecules free from the broad O-H region peak, indicating no or almost no presence of water (H_2O) in the filament.

Acknowledgement

We want to sincerely thank Universiti Teknikal Malaysia Melaka (UTeM) for their generous financial support, which covered the publication fee and the facilities provided for the research.

References

[1] Fang, Lichen, Yishu Yan, Ojaswi Agarwal, Shengyu Yao, Jonathan E. Seppala and Sung Hoon Kang. "Effects of environmental temperature and humidity on the geometry and strength of polycarbonate specimens prepared by fused filament fabrication." *Materials* 13, no. 19 (2020): 4414. https://doi.org/10.3390/ma13194414

[2] Alamri, Hatem and It Meng Low. "Effect of water absorption on the mechanical properties of nano-filler reinforced epoxy nanocomposites." *Materials & Design* 42 (2012): 214-222. https://doi.org/10.1016/j.matdes.2012.05.060

[3] Algarni, Mohammed. "The influence of raster angle and moisture content on the mechanical properties of PLA parts produced by fused deposition modeling." *Polymers* 13, no. 2 (2021): 237. https://doi.org/10.3390/polym13020237

[4] Titone, Vincenzo, Antonio Correnti and Francesco Paolo La Mantia. "Effect of moisture content on the processing and mechanical properties of a biodegradable polyester." *Polymers* 13, no. 10 (2021): 1616. https://doi.org/10.3390/polym13101616

[5] Kwon, SoonWon, SeonWoo Lee, YongRae Kim, YoungChan Oh, SunKon Lee, JooHyung Kim and JangWoo Kwon. "A Filament supply system capable of remote monitoring and automatic humidity control for 3D printer." *Journal of Sensors* 2020, no. 1 (2020): 8846466. https://doi.org/10.1155/2020/8846466

[6] Hamid, Rahimah Abdul, Fatima Hanem Hamezah and Jeefferie Abd Razak. "Influence of humidity on the tensile strength of 3D printed PLA filament." In *Symposium on Intelligent Manufacturing and Mechatronics*, pp. 497-502. Singapore: Springer Nature Singapore, 2021. https://doi.org/10.1007/978-981-16-8954-3_47

[7] Akhoundi, Behnam, Mojtaba Nabipour, Faramarz Hajami and Diana Shakoori. "An experimental study of nozzle temperature and heat treatment (annealing) effects on mechanical properties of high-temperature polylactic acid

in fused deposition modeling." *Polymer Engineering & Science* 60, no. 5 (2020): 979-987. https://doi.org/10.1002/pen.25353

[8] Hamat, Sanusi, Mohamad Ridzwan Ishak, Mohd Sapuan Salit, Noorfaizal Yidris, Syamir Alihan Showkat Ali, Mohd Sabri Hussin, Maliki Ibrahim and Asmawi Sanuddin. "Tensile Properties of 3D Printed Recycled PLA Filament: A Detailed Study on Filament Fabrication Parameters." *Journal of Advanced Research in Applied Mechanics* 110, no. 1 (2023): 63-72. https://doi.org/10.37934/aram.110.1.6372

[9] Abeykoon, Chamil, Pimpisut Sri-Amphorn and Anura Fernando. "Optimization of fused deposition modeling parameters for improved PLA and ABS 3D printed structures." *International Journal of Lightweight Materials and Manufacture* 3, no. 3 (2020): 284-297. https://doi.org/10.1016/j.ijlmm.2020.03.003

[10] Afonso, João Araújo, Jorge Lino Alves, Gabriela Caldas, Barbara Perry Gouveia, Leonardo Santana and Jorge Belinha. "Influence of 3D printing process parameters on the mechanical properties and mass of PLA parts and predictive models." *Rapid Prototyping Journal* 27, no. 3 (2021): 487-495. https://doi.org/10.1108/RPJ-03-2020-0043

[11] Chacón, Jesus Miguel, Miguel Angel Caminero, Eustaquio García-Plaza and Pedro J. Núnez. "Additive manufacturing of PLA structures using fused deposition modelling: Effect of process parameters on mechanical properties and their optimal selection." *Materials & Design* 124 (2017): 143-157. https://doi.org/10.1016/j.matdes.2017.03.065

[12] Patel, Kautilya S., Dhaval B. Shah, Shashikant J. Joshi, Faisal Khaled Aldawood and Mohamed Kchaou. "Effect of process parameters on the mechanical performance of FDM printed carbon fiber reinforced PETG." *Journal of Materials Research and Technology* 30 (2024): 8006-8018. https://doi.org/10.1016/j.jmrt.2024.05.184

[13] Hamid, Rahimah Abdul, Siti Nur Hidayah Husni and Teruaki Ito. "Effect of Printing Orientation and Layer Thickness on Microstructure and Mechanical Properties of PLA Parts." *Malaysian Journal on Composites Science and Manufacturing* 8, no. 1 (2022): 11-23. https://doi.org/10.37934/mjcsm.8.1.1123

[14] Bhandari, Sunil, Roberto A. Lopez-Anido and Douglas J. Gardner. "Enhancing the interlayer tensile strength of 3D printed short carbon fiber reinforced PETG and PLA composites via annealing." *Additive Manufacturing* 30 (2019): 100922. https://doi.org/10.1016/j.addma.2019.100922

[15] Shuto, Rei, Sawane Norimatsu, Dwayne D. Arola and Ryosuke Matsuzaki. "Effect of the nozzle temperature on the microstructure and interlaminar strength in 3D printing of carbon fiber/polyphenylene sulfide composites." *Composites Part C: Open Access* 9 (2022): 100328. https://doi.org/10.1016/j.jcomc.2022.100328

[16] Hsueh, Ming-Hsien, Chao-Jung Lai, Shi-Hao Wang, Yu-Shan Zeng, Chia-Hsin Hsieh, Chieh-Yu Pan and Wen-Chen Huang. "Effect of printing parameters on the thermal and mechanical properties of 3d-printed pla and petg, using fused deposition modeling." *Polymers* 13, no. 11 (2021): 1758. https://doi.org/10.3390/polym13111758

[17] Birosz, Marton Tamas, Daniel Ledenyak and Matyas Ando. "Effect of FDM infill patterns on mechanical properties." *Polymer Testing* 113 (2022): 107654. https://doi.org/10.1016/j.polymertesting.2022.107654

[18] Ning, Jinqiang, Daniel E. Sievers, Hamid Garmestani and Steven Y. Liang. "Analytical modeling of part porosity in metal additive manufacturing." *International Journal of Mechanical Sciences* 172 (2020): 105428. https://doi.org/10.1016/j.ijmecsci.2020.105428

[19] Ayrilmis, Nadir. "Effect of layer thickness on surface properties of 3D printed materials produced from wood flour/PLA filament." *Polymer testing* 71 (2018): 163-166. https://doi.org/10.1016/j.polymertesting.2018.09.009

[20] Qiu, Jun, Seddik Khalloufi, Alex Martynenko, Gerard Van Dalen, Maarten Schutyser and Cristhian Almeida-Rivera. "Porosity, bulk density and volume reduction during drying: Review of measurement methods and coefficient determinations." *Drying Technology* 33, no. 14 (2015): 1681-1699. https://doi.org/10.1080/07373937.2015.1036289

[21] Al-Maharma, Ahmad Y., Sandeep P. Patil and Bernd Markert. "Effects of porosity on the mechanical properties of additively manufactured components: a critical review." *Materials Research Express* 7, no. 12 (2020): 122001. https://doi.org/10.1088/2053-1591/abcc5d

[22] Keleş, Özgür, Eric H. Anderson, Jimmy Huynh, Jeff Gelb, Jouni Freund and Alp Karakoç. "Stochastic fracture of additively manufactured porous composites." *Scientific reports* 8, no. 1 (2018): 15437. https://doi.org/10.1038/s41598-018-33863-4